J Mater Sci (2006) 41:5029–5032
DOI 10.1007/s10853-006-0125-5

LETTER

Effect of the addition of CaO–MgO–SiO$_2$ glass on the sintering and mechanical properties of Al$_2$O$_3$/3Y-TZP composites

X. W. Huang · J. C. Yu · F. Ding

Received: 25 October 2005 / Accepted: 14 December 2005 / Published online: 27 May 2006

It is well known that the higher mechanical properties of Al$_2$O$_3$/3Y-TZP composites are mainly associated with the stress-induced transformation toughening and microcrack toughening [1–3]. However, in the system of Al$_2$O$_3$/ZrO$_2$, the components have a limited mutual solubility and possess a grain-growth inhibition for each other [4, 5]. As a result, pressureless sintering of Al$_2$O$_3$/3Y-TZP composites was performed at higher temperatures, or in most cases pressure-aided sintering (hot-pressing or hot-isostatic pressing) was applied to facilitate the densification [6, 7]. For the purpose of production cost, it is desirable to sinter Al$_2$O$_3$/3Y-TZP composites pressurelessly at a lower temperature, which is of higher performance.

A variety of additives have been found to be effective in the sintering of ZrO$_2$, such as CuO, B$_2$O$_3$, TiO$_2$ and Mn$_2$O$_3$ [8–11]. It was also found that the densification of alumina was greatly enhanced by the addition of TiO$_2$–MnO$_2$, and the microstructure development was characterized by their promotion to the grain growth [12–14].

However, fewer reports appeared in the literature about the sintering of Al$_2$O$_3$/3Y-TZP composites at lower temperature, and the effect of additives on the mechanical properties of the composites remains unknown. The purpose of present work is to densify Al$_2$O$_3$/3Y-TZP composites by pressureless sintering with the addition of CaO–MgO–SiO$_2$ glass (CMS) and to investigate the effect of the glass on the sintering and mechanical properties of the composites.

Analytical reagent grade CaCO$_3$, MgCO$_3$ and SiO$_2$ were melted to form a ternary glass having a composition of 30.0 wt% CaO, 9.0 wt% MgO and 61.0 wt% SiO$_2$. The glass was crushed and attrition milled in distilled water using alumina balls as milling medium. After being dried, the glass powder was sieved through 120 mesh. Pellet of the CMS glass powder was pressed in cylindrical shape and then heated to 1,450 °C. Melting behavior of the CMS glass was observed by optical microscope, the softening point and the melting point were 1,207 °C and 1,311 °C, respectively. For the final product of Al$_2$O$_3$/3Y-TZP composites, high purity commercial α-Al$_2$O$_3$ and 3Y-TZP were weighed and mixed according to the composition listed in Table 1, then CMS glass was added into the mixed powder (the weight ratio of CMS glass to mixed powder was 2:98) and milled for 24 h. The composite powders were uniaxially dry pressed at 50 MPa, followed by cold isostatic pressing at 200 MPa. Samples were heated at 5 °C/min to the final sintering temperatures (1,350 °C–1,550 °C), held for 2 h, and finally cooled with the furnace. Bulk density was measured using the Archimedes method. The samples were machined into dimensions of 3 mm × 4 mm × 35 mm. Bending strength was measured by the three-point method with a span of 30 mm and a cross-head speed of 0.5 mm/min. At least five samples were tested. The fracture toughness measurement was carried out on the polished surface by microindentation method using Shetty's equation [15]:

$$K_{IC} = 0.0937(H_V P/4l)^{1/2}$$

where H_V is the Vicker's hardness, P is the load, l is the crack length from an indentation corner to its corresponding crack tip.

X. W. Huang (✉) · J. C. Yu
College of Materials Science and Engineering, Fuzhou University, Fuzhou 350002, China
e-mail: xwhuang@fzu.edu.cn

F. Ding
College of Geographical Sciences, Fujian Normal University, Fuzhou 350007, China

Table 1 Composition for the preparation of Al_2O_3/3Y-TZP composites

Samples	Composition		
	α-Al_2O_3 (vol%)	3Y-TZP (vol%)	CMS glass (wt%)
AZ15(2)	15	85	2
AZ30(2)	30	70	2
AZ70(2)	70	30	2
AZ85(2)	85	15	2

X-ray diffraction (XRD) was used to determine the phases presented in the samples. The phase composition was calculated according to the method of Miller et al. [16] using the following expressions:

$$\frac{X_m}{X_{c,t}} = 0.82\frac{I_m(11\bar{1}) + I_m(111)}{I_{c,t}(111)}$$

$$\frac{X_c}{X_t} = 0.88\frac{I_c(400)}{I_t(400) + I_t(004)}$$

The microstructure of the sintered bodies was observed by scanning electron microscopy (SEM) on the polished and thermally etched surfaces.

Relative densities of the composites as a function of sintering temperature were plotted in Fig. 1. For the purpose of comparison, the curve of sample AZ70 without additives was also given. Calculations of the relative densities were based on the theoretical values of 6.08 g/cm^3 for 3Y-TZP, 3.98 g/cm^3 for Al_2O_3, and 2.687 g/cm^3 for CMS glass, respectively. Densification of the composites was greatly enhanced by the addition of CMS glass. The mechanism associated with this process was attributable to liquid phase sintering caused by the formation of a eutectic liquid among CaO, MgO and SiO_2 at sintering temperatures.

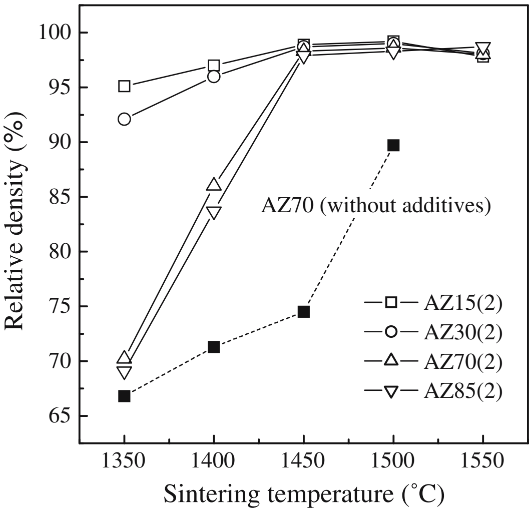

Fig. 1 Relative density as a function of sintering temperature for Al_2O_3/3Y-TZP composites

As shown in Fig. 1, the samples with higher Al_2O_3 content exhibited lower densification when sintering was carried out between 1,350 °C and 1,450 °C, which was also observed in previous investigations [17, 18]. Although numerous research studies concerning the densification of Al_2O_3/ZrO_2 composites have been conducted, discrepancy still exists in the explanation of densification retard mechanism by Al_2O_3 [19–21]. In the present study, it was found that the densification of Al_2O_3 was more difficult than that of 3Y-TZP. With the addition of 2 wt% CMS glass, 3Y-TZP could be densified at a temperature as low as 1,400 °C, however, at the same temperature, Al_2O_3 achieved only a relative density of 85.3%. A possible reason for this result might be the different starting powder particle sizes (0.7 μm and 0.2 μm for Al_2O_3 and 3Y-TZP, respectively).

Differences in the densification retard effect, arising from the different Al_2O_3 contents, became negligibly small at higher sintering temperatures. Maximum density was reached at 1,500 °C for samples AZ15(2), AZ30(2) and AZ70(2). Temperature as high as 1,550 °C was needed for sample AZ85(2) to obtain maximum density.

Microstructural differences caused by the composition and sintering temperature were illustrated in Fig. 2. The dark and bright contrasts in the scanning electron micrographs were Al_2O_3 and ZrO_2 grains, respectively. Dispersion of the grains in the microstructure was predominantly intergranular with a few being intragranular. Mean grain sizes, which varied from submicron to several microns, increased steadily with the sintering temperature. The grain growth inhibition for both Al_2O_3 and ZrO_2 was obvious when comparing Fig. 2b with Fig. 2c.

Small amount of larger cubic ZrO_2 (c-ZrO_2) grains were also observed in the microstructure. The uneven distribution of Y_2O_3 in ZrO_2 grains, which resulted from the existence of grain boundary phase, was responsible for the formation of cubic grains. Detailed reports could be found in previous paper [22].

XRD patterns, as given in Fig. 3, revealed that the phase assembly existed in the composites were mainly α-Al_2O_3, t-ZrO_2 and c-ZrO_2. Only a tiny amount of m-ZrO_2 was observed when sintered at 1,450 °C. No other different phases were detected.

Because of the peak overlap of t-ZrO_2 and c-ZrO_2, as shown in Fig. 3, calculation of c-ZrO_2 content was conducted using the high angle diffraction peak intensity. The results were shown in Table 2. It could be seen that c-ZrO_2 existed in all samples when sintering was carried out between 1,400 °C and 1,550 °C, and its content increased

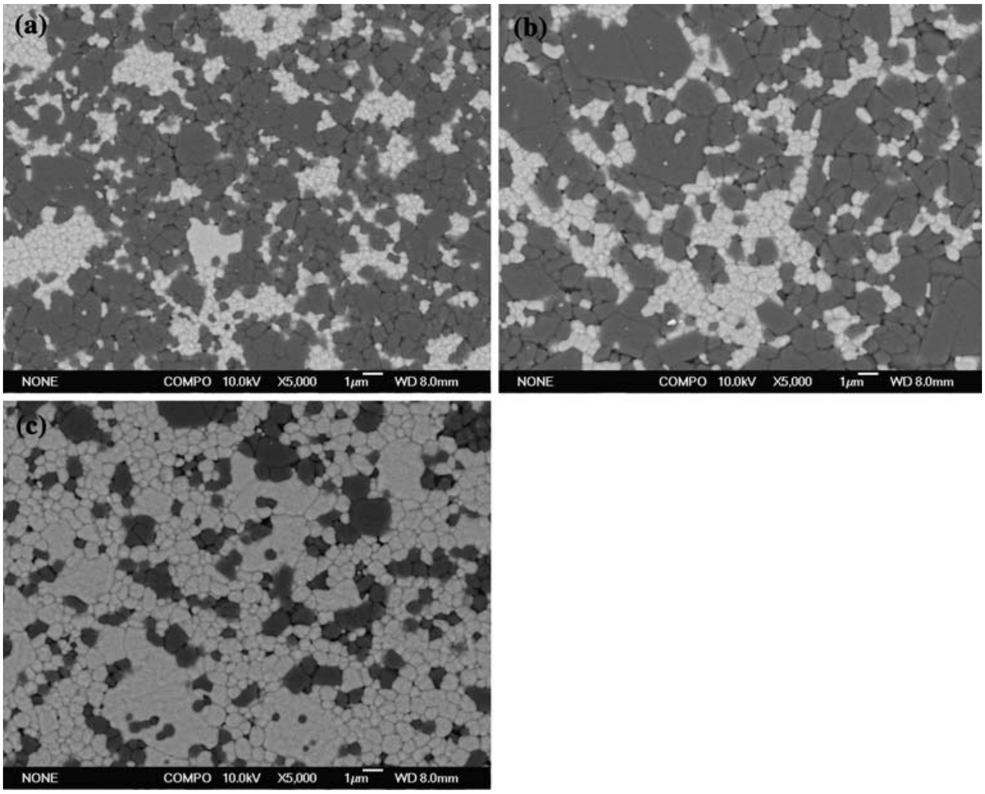

Fig. 2 SEM micrographs for sample AZ70(2) sintered at (**a**) 1,450 °C, (**b**) 1,500 °C, and (**c**) sample AZ30(2) sintered at 1,500 °C

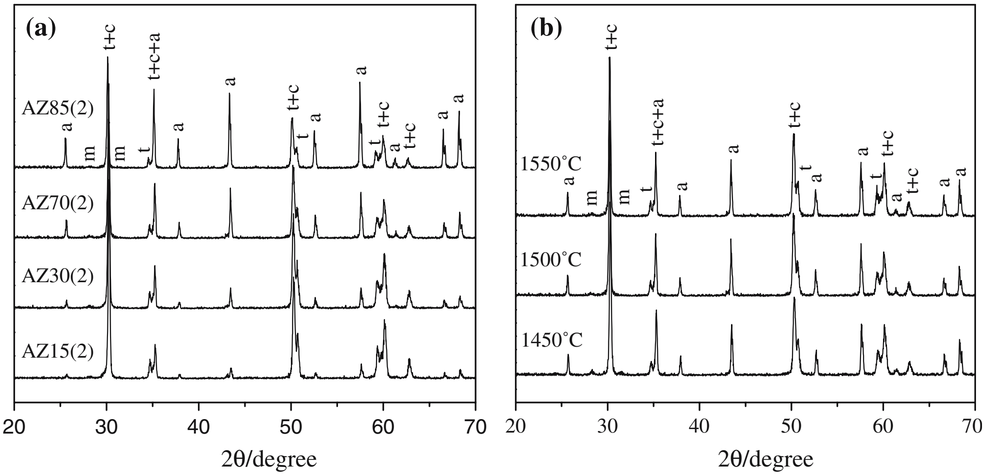

Fig. 3 XRD patterns for (**a**) Al_2O_3/3Y-TZP composites sintered at 1,500 °C, and (**b**) sample AZ70(2) sintered at different temperatures

gradually with the sintering temperature. However, it seemed that Al_2O_3 content had no obvious effects on the formation of cubic phase.

Table 2 Calculation results of c-ZrO2 content for Al_2O_3/3Y-TZP composites

Samples	Content of c-ZrO2 (%)		
	1,450 °C	1,500 °C	1,550 °C
AZ15(2)		19.0	
AZ30(2)		17.9	
AZ70(2)	17.0	18.2	18.7
AZ85(2)		17.7	

Bending strength and fracture toughness as a function of sintering temperature were given in Figs. 4 and 5, respectively. Samples with higher ZrO_2 content achieved higher strength and toughness. Maximum strength was attained at 1,500 °C for the samples denoted as AZ15(2), AZ30(2), AZ70(2), and 1,550 °C for sample AZ85(2), owing to their respective maximum densities at corresponding temperatures. Maximum toughness was obtained for all samples when sintered at 1,550 °C.

In conclusion, Al_2O_3/3Y-TZP composites with the addition of CMS glass could be densified at a lower temperature when compared with solid state sintering. Simultaneously, finer grain microstructure as well as higher content of

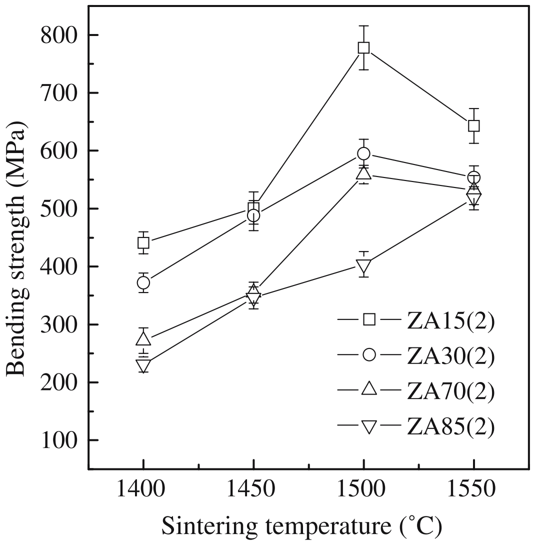

Fig. 4 Bending strength as a function of sintering temperature for Al_2O_3/3Y-TZP composites

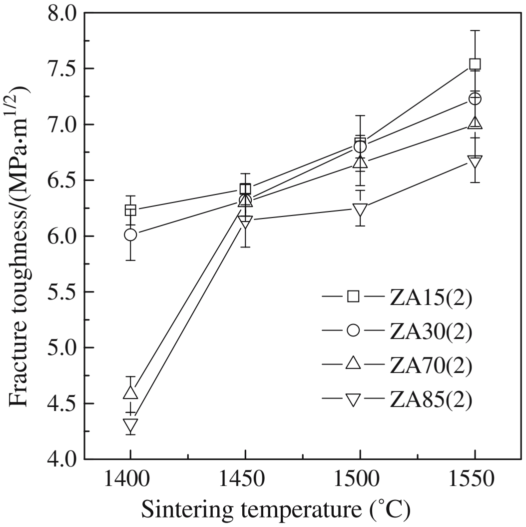

Fig. 5 Fracture toughness as a function of sintering temperature for Al_2O_3/3Y-TZP composites

t-ZrO_2, resulted from the lower sintering temperature, was beneficial to the improvement of mechanical properties.

Acknowledgements This research was sponsored by the funds from Fujian Provincial Department of Science & Technology (No. 2004J006) and Fuzhou University (No. 2003-XQ-02). The author is also grateful to Prof. S. W. Wang and Prof. X. X. Huang (Shanghai Institute of Ceramics, Chinese Academy of Sciences) for their generous financial support and constructive advice.

References

1. Lange FF (1982) J Mater Sci 17:225
2. Claussen N (1978) J Am Ceram Soc 61:85
3. Evans AG, Heuer AH (1980) J Am Ceram Soc 63:241
4. Lange FF, Hirlinger MM (1984) J Am Ceram Soc 67:164
5. Lange FF, Hirlinger MM (1987) J Am Ceram Soc 70:827
6. Leriche A, Moortgat G, Cambier F, Homerin P, Thevenot F, Orange G, Fan-Tozzi G (1992) J Eur Ceram Soc 9:169
7. Chaim R (1992) J Mater Sci 27:5597
8. Lawson S, Gill C, Dransfield GP (1995) J Mater Sci 30:3057
9. Buchanan RC, Sircar A (1983) J Am Ceram Soc 67:C-20
10. Radford KC, Bratton RJ (1979) J Mater Sci 14:59
11. Kimura N, Okamura H, Morishita J (1988) In: Somiya S, Yamamoto N, Yanahida H (eds) Advances in ceramics, science and technology of zirconia III, vol 24. American Ceramic Society, Columbus, OH, p 183
12. Cutler IB, Bradshaw C, Christensen CJ, Hyatt EP (1957) J Am Ceram Soc 40:134
13. Erkalfa H, Misirli Z, Baykara T (1998) Ceram Int 24:81
14. Pereira SR, Sepulveda P, Pandolfelli VC (1999) Interceram 48:238
15. Shetty DK, Wright IG, Mincer PN, Clauer AH (1985) J Mater Sci 20:1873
16. Miller RA, Smialek JL, Garlick RG (1981) Adv Ceram 3:241
17. Shi JL, Gao JH, Li BS, Yen TS (1995) J Eur Ceram Soc 15:967
18. Upadhyaya DD, Dalvi PY, Dey GK (1993) J Mater Sci 28:6103
19. Nakada Y, Kimura T (1997) J Am Ceram Soc 80:401
20. Shi JL, Yen TS (1995) J Eur Ceram Soc 15:363
21. Tuan WH, Brook RJ (1989) J Mater Sci 24:1953
22. Huang XW, Yu JC, Li Q, Huang XX, Li XQ, Liu XL (2005) J Mater Sci 40:1693